HHS Public Access

Author manuscript

Toxicol In Vitro. Author manuscript; available in PMC 2019 December 19.

Published in final edited form as:

Toxicol In Vitro. 2019 December ; 61: 104628. doi:10.1016/j.tiv.2019.104628.

An in vitro depth of injury prediction model for a histopathologic classification of EPA and GHS eye irritants☆

Stewart Lebrun[a,*], **Yilu Xie**[b], **Sara Chavez**[a], **Roxanne Chan**[a], **James V. Jester**[b]

[a]Lebrun Labs LLC, Anaheim, CA, United States of America

[b]Gavin Herbert Eye Institute, University of California, Irvine, CA, United States of America

Abstract

The purpose of this study was to develop Globally Harmonized System (GHS) and U.S. Environmental Protection Agency (EPA) prediction models for classifying irritant materials based on histopathologic in vitro depth of injury (DoI) measurements. Sixteen different materials were selected, representing all classes of toxicity, according to the GHS and EPA classification systems. Food-source rabbit eyes, similar to eyes used for the widely accepted Bovine Corneal Opacity and Permeability and Isolated Chicken Eye ocular irritation tests, were used. Tissues were exposed to test material for 1 min, and corneas were collected at 3-and 24-hours post-exposure. Tissues were then fixed and processed for live/dead biomarker fluorescent staining using phalloidin. DoI was then measured, and the percent DoI values for the epithelium and stroma were compared to the EPA and GHS classifications. Excluding surfactants, EPA nonclassified (category IV) materials showed no stromal and very slight epithelial damage (≤10%) to the cornea, whereas EPA corrosive (category I) materials showed significantly greater damage ($P < 0.001$), ranging from 39% to 100% of the stromal depth. Importantly, EPA reversible (categories II and III) materials showed significant damage to the epithelium (> 10%, $P < 0.005$) but significantly less severe damage to the corneal stroma ($P < 0.001$), ranging from 1% to 38% of the stromal depth. GHS nonclassified (category NC) irritants caused damage to the epithelium but not to the stroma. All GHS class 2 materials showed damage to the stroma (1–11%), whereas GHS corrosives caused significantly greater damage to the stroma (38–100%; $P < 0.001$). Additionally, one corrosive material, which produced a stromal DoI of 99% at 24 h, produced no apparent damage at 3-hours post-exposure. Based on these findings, histopathologic EPA and GHS prediction models are proposed that appear to separate and identify reversible irritants from other irritant classes. Furthermore, GHS classification appears to require stromal damage, whereas NC materials may or may not damage the corneal epithelium.

Keywords

Ocular irritation; In vitro eye irritation tests; Isolated rabbit eye; Depth of injury; Cornea; EPA; GHS

[*]Corresponding author at: Lebrun Labs LLC, 3301 E. Miraloma Ave., Ste. 194, Anaheim, CA 92806, United States of America. SJ@lebrunlabs.com (S. Lebrun).

1. Introduction

Ocular irritation testing is important for the identification of chemicals or mixtures that cause ocular adverse effects and is routinely conducted to ensure that materials are appropriately classified, labeled, and meet regulatory and safety guidelines (Bruner, 1992). Currently, the in vivo Draize rabbit eye test is the recognized, standard ocular irritation test; it uses a clinical scoring system that grades the severity of irritation based on external effects to the cornea, iris, and conjunctiva as determined by a threshold response to the cornea, iris, or conjunctiva, and then the number of days until effects cannot be observed in the live rabbit eye. Based on these responses, chemicals are classified using either the Globally Harmonized System (GHS) or the U.S. Environmental Protection Agency (EPA) classifications. The GHS classification includes the classes nonclassified (NC), 2 (reversible irritation), and 1 (irreversible irritation or extreme damage), which refer to effects on the eyes, whereas the EPA classification system includes: I (corrosive), II (reversible by 21 days after exposure), III (reversible by 7 days after exposure), and IV (no significant damage 24 h after exposure) (UN, 2011).

While in the past, the in vivo Draize test was routinely used to determine a material's irritation potential, it has been widely criticized for its inconsistency, lack of reproducibility, and limited ability to predict materials that are toxic to the human eye (Bruner, 1992; Rowan, 1984; Weil and Scala, 1971). Furthermore, there is widespread public opinion against the use of animals for routine product testing, and more importantly, there are bans or severe limitations on the use of animals for product testing in a wide range of countries (Senate Joint Resolution 22, 2014; Humane Society, 2017). At present, legislation in the U.S. proposes to ban the use of animals for a wide range of testing applications (H.R.2790, 2017), while at the same time requiring EPA to evaluate all existing and new chemicals for unreasonable risk of injury to human health or the environment (S.697, 2015). In addition, the California Cruelty-Free Cosmetics Act (SB 1249) would make California, on or after January 1, 2020, the first state in the U.S. to ban the sale of cosmetics if animal testing is used to determine the safety of the product or its formulation by the manufacturer or its suppliers (SB1249, 2018).

In light of these issues, increased interest has focused on the development of nonanimal testing methods and strategies to replace the Draize test. Toward this end, the Interagency Coordinating Committee for the Validation of Alternative Methods (ICCVAM) and the European Centre for Validation of Alternative Methods (ECVAM) conducted retrospective evaluations of data available for four organotypic methods and four cytotoxicity and cell function methods. Based on these retrospective evaluations, the predictive performance of all individual test methods was not felt to be sufficient for any one test, or group of tests, to fully replace the rabbit Draize eye test (ICCVAM, 2009). ICCVAM and ECVAM did, however, accept the Bovine Cornea Opacity and Permeability (BCOP) test, Isolated Chicken Eye (ICE) test, Cytosensor Microphysiometer (CM, for water-soluble materials), and fluorescein leakage test (FLT, for water-soluble materials) as screening tests for the identification of materials not requiring classification (NC), ocular corrosives, and severe eye irritants, and the CM as a screening test for the identification of materials not classified for eye irritation (surfactants and surfactant mixtures). Recently, differentiated cell culture

models, including the EpiOcular™ Eye Irritation Test, the SkinEthic™ Human Corneal Epithelium (HCE), and the LabCyte™ CORNEA-MODEL24, were demonstrated to have utility for the detection of NC (OECD, 2018b). The in chemico test OptiSafe™ (developed by one of the authors) was also shown to have utility for the detection of EPA IV and I, and GHS NC and 1 materials (Choksi et al., 2017; Lebrun et al., 2019; Vij et al., 2019). However, no single test, or combination of tests, can currently detect reversible irritation with any degree of statistical certainty (Wilson et al., 2015).

To address the predictive performance of ex vivo methods that use food-source animal eyes, ICCVAM made specific recommendations for improvement, including the addition of measuring depth of injury (DoI) as an endpoint in the BCOP and ICE tests, and has more recently published guidelines for the collection, processing, and histopathologic analysis of eye tissues (OECD, 2018a).

We have performed a histopathologic, live biomarker analysis of a rabbit eye irritation test using a masked set of 16 materials of differing EPA (categories I–IV) and GHS (classes 1, 2, and NC) classifications based on historical Draize test data. We report that this method performed at 24-hours post-exposure can distinguish three different groups of materials, including nonirritants (EPA IV/GHS NC), corrosives (EPA I/GHS 1), and reversible irritants (EPA II/III, GHS 2). The new DoI procedures and prediction models associate regulatory classifications with specific histopathologic endpoints.

2. Methods

2.1. Rabbit eyes

Since historical Draize test data are based on live rabbit ocular responses, rabbit eyes represent the most relevant test matrix. In addition, there are significant similarities between rabbit eyes and human eyes, which were likely factors in why rabbits were originally selected as animal models for ocular testing (Draize et al., 1944). Enucleated rabbit eyes with intact eyelids that protect the corneal surface were obtained from food-source rabbits, placed in Hank's balanced salt solution (pH 7.4), and shipped overnight on ice (Pel-Freez Biologicals, Rogers, AR). After surgical removal of the eyelids and ocular muscles, the epithelial integrity was examined by applying a 0.25% solution of Lissamine™ Green B (Sigma Aldrich, St. Louis, MO) to the cornea to stain the surface corneal epithelium (Hamrah et al., 2011). Eyes were then rinsed with phosphate-buffered saline (PBS), and green staining of the corneal surface was observed using a dissecting microscope. Stained corneas were excluded from the study. Intact eyes were placed in a 12-well cell culture plate (Costar 3513, Corning Inc., Corning, NY), containing approximately 1 mL sterile cell culture media. Plates were then placed in a humidified, CO_2 incubator at 37 °C for 2 h.

2.2. Test materials and material application

Test materials, concentrations, and text abbreviations are listed in Table 1, and distilled, deionized, sterile water served as a control. Materials were selected based on the availability of historical in vivo data. (ECETOC, 1998; Gautheron et al., 1994; Grune et al., 2000). Individual materials were placed in coded vials and overlaid with argon gas. Handling of test

materials was conducted under a standard fume hood to avoid personnel exposure. Decoding of materials was not performed until after material testing and during analysis of the data.

Exposure of corneas to test materials was conducted under a standard laboratory fume hood. Eyes were initially placed on a customized eye holder, with the cornea facing up, and an 8-mm internal dosing ring was placed over the central cornea. Test materials (100 μL) were then pipetted into the ring, and the cornea was exposed for 1 min. The material was then removed using a pipette and safely discarded, and the eye was rinsed with 20 mL sterile wash buffer. Eyes were then returned to the 12-well plates. For 3-h post-exposure times, intact eyes were placed back into the humidified incubator for 3 h, and then removed and the corneas collected, fixed, and processed for fluorescent labeling, as described below. For 24-hours post-exposure, corneas without the iris or lens were removed and placed on custom posts (Fig. 1). Sterile medium was then added to the dish up to the limbus. Corneas were then placed in a humidified incubator for 24 h. The next day, corneas were placed in fixative and later processed for fluorescent labeling.

2.3. Tissue processing and fluorescent labeling

Briefly, corneal tissue blocks were embedded in O.C.T. Compound (Tissue-Teck, Sakura Finetek, Torrance, CA), snap frozen in liquid nitrogen, and stored in an ultralow freezer (−80 °C, Revco Ultima II, Asheville, NC) before sectioning with a Leica CM 1850 cryotome (Leica, Wetzlar, Germany). Nine 8-μm-thick tissue sections were collected at 100-μm intervals and placed onto glass slides, alternating between slides so that the greatest depth of sampling was achieved (three sections/slide). Sections on one slide were then stained with Alexa 488-labeled phalloidin (Invitrogen, Eugene, OR) for 20 min. Slides were washed three times for 5 min each, counterstained with DAPI (300 nM, Invitrogen) in PBS for 15 min, and then washed for a final 5 min. Coverslips were then added to the slides using Gel/Mount (Biomeda, Foster City, CA) mounting media.

2.4. Data collection and analysis

Stained sections were viewed using a Leica DMI6000B fully auto-mated inverted fluorescence microscope (Leica Microsystems Inc., Buffalo Grove, IL). Tiled images over the corneal tissue section were collected using a low-light-level camera (QIClick, QImaging, British Columbia, Canada) and Leica 20× HC Plan Apo, 0.75 NA objective. Images were then stitched using Meta Imaging Series software (Molecular Devices, Downington, PA). To measure DoI, the epithelial thickness, stromal thickness, and stromal DoI were measured at 500-μm intervals along the image of the tissue section using Metamorph Imaging Processing software (Molecular Devices). To assess stromal DoI, the thickness of the dead stroma that did not stain with phalloidin was also measured. Epithelial DoI was then determined by calculating the difference between the treated and control corneal epithelial thicknesses. Similarly, stromal DoI was determined by calculating the percentage of stromal damage by dividing the measured stromal DoI by the stromal thickness. An average epithelial and stromal DoI was then calculated for each section, and the average of three sections was recorded for each eye. Only one slide (three sections) was evaluated, and the remaining slides saved for future evaluation if necessary.

2.5. Statistics

Data were statistically analyzed using SigmaStat for Windows 3.11 (Systat Software Inc., Point Richmond, CA). Differences between materials based on EPA and GHS classifications for effects on epithelial and stromal DoI over time were detected using a two-way analysis of variance and the All Pairwise Multiple Comparisons test (Hom-Sidek method).

3. Results

3.1. Assessment of DoI in isolated rabbit eyes

As shown in Fig. 2A, water-treated, control rabbit corneas treated with phalloidin (green = phalloidin; red = nuclei; DAPI staining was pseudo-colored red to enhance contrast) showed staining of both the corneal epithelium (Epi), stromal keratocytes (Stroma), and corneal endothelium (Endo). In the corneal epithelium (Fig. 2A, inset), phalloidin strongly stained the stratified, 5–7-cell-thick, epithelial layer, which averaged 36.4 ± 5.8 μm and 38.8 ± 4.4 μm in thickness in the 3 hour and 24 hour post-exposure rabbit corneas, respectively (Tables 2 and 3). In the stroma, phalloidin stained the cell bodies of stromal keratocytes that were uniformly distributed throughout the corneal stroma (double-headed arrow), which averaged 348.2 ± 48.5 μm and 358.4 ± 22.0 μm in the 3 hour and 24 hour post-exposure corneas, respectively (Tables 2 and 3).

In contrast, rabbit corneas exposed to known hazardous ocular irritants showed substantial damage to both the corneal epithelium and stroma. As shown in Fig. 2B, moving from the limbal region (Limbus) toward the central cornea, an abrupt change in epithelial and stromal phalloidin staining could be detected (large arrow), delineating the edge of the treatment zone defined by the dosing ring placed onto the corneal surface to limit exposure of materials to the central 8 mm of the cornea. Moving more centrally, stromal DoI, indicated by the double-headed arrows, appeared to increase slightly in thickness, achieving a maximum depth within the central 4–6 mm. As shown in the inset, unlike water-treated corneas, corneas treated with hazardous materials showed a complete loss of stromal and epithelial phalloidin staining, indicative of cell death.

3.2. Effects of ocular irritants on isolated rabbit corneas

A total of 16 different materials were tested (Table 1), representing the four EPA and three GHS classifications (discussed below) based on historical Draize data (Barroso et al., 2017; ECETOC, 1998). Except for tetraethylene glycol diacrylate, all EPA I materials showed extensive stromal damage at both 3-and 24-hours post-exposure, with stromal DoI ranging from 25% to 100% at 3 h, and 38% to 100% at 24 h (Fig. 3, Tables 2 and 3). Epithelial DoI was more variable at 3 h, ranging from −1% to 100%, but was more consistent at 24 h (all 100%). Interestingly, tetraethylene glycol diacrylate showed 0% stromal DoI at 3 h (Fig. 3, A_1) but 99% stromal DoI at 24 h (Fig. 3, A_2). Furthermore, the rabbit corneal epithelium appeared more resistant to tetraethylene glycol diacrylate injury than the stroma, exhibiting only a 15% epithelial DoI compared to the 99% stromal DoI at 24 h. Epithelial survival was also noted for cyclohexane, which showed a −1% epithelial DoI at 3 h compared to a 100% epithelial DoI at 24 h (Fig. 3, B_1 and B_2).

As shown in Fig. 4 and Tables 2 and 3, rabbit eyes treated with EPA II materials showed less stromal DoI than EPA I materials (except for the surfactant Triton X-100), ranging from 1% to 22% at 3 h and 1% to 38% at 24 h. Similarly, epithelial DoI was generally less than for EPA I materials and ranged from −5% to 23% at 3 h, and 12% to 100% at 24 h. Overall, there appeared to be greater damage measured at 24 h compared to 3 h for EPA II materials. By comparison, Triton X-100 showed extensive stromal damage at both 3 and 24 h, averaging 99% and 100%, respectively (Fig. 4, B_1 and B_2). However, like the other EPA II materials, the recorded epithelial DoI was much greater at 24 h, averaging 100%, compared to 3 h, which averaged only 21%.

DoI for EPA III materials is shown in Fig. 5 (Tables 2 and 3); three of four materials showed some stromal DoI, ranging from 2% to 11% at 3 h, and 1% to 12% at 24 h, which appeared to be slightly less or similar to values measured for EPA II materials. Similarly, epithelial DoI appeared less extensive and ranged from 10% to 45% at 3 h, and 16% to 100% at 24 h. Tween 20, however, showed no stromal DoI at either 3 or 24 h after exposure (Fig. 5, C_1 and C_2). Epithelial DoI was also not detected, averaging 2% at 3 h and only 16% at 24 h.

As shown in Fig. 6 (Tables 2 and 3), no EPA IV materials produced any stromal DoI at either 3-or 24-hours post-exposure. Similarly, epithelial DoI was not detected, ranging from 3% to 14% at 3 h, and −15% to 10% at 24 h.

3.3. Comparison of DoI between EPA and GHS categories

Comparison between materials for epithelial and stromal DoI are presented in Fig. 7. As shown for epithelial DoI (Fig. 7A), no EPA IV materials showed any damage to the corneal epithelium, and the measured epithelial DoI was significantly less than that detected for all other categories, including EPA I ($P < 0.001$), EPA II ($P < 0.005$), and EPA III ($P < 0.005$) (Table 4). Furthermore, the measured epithelial thickness, while significantly different than the other categories, was not significantly different to control corneas at either 3 or 24 h after exposure, nor were there any apparent effects of exposure time on epithelial thickness. Stromal DoI was significantly less than that measured in eyes exposed to both EPA I ($P < 0.001$) and EPA II ($P < 0.005$) materials (Fig. 7B and Table 4), whereas the measured stromal thickness was not significantly different from that of control eyes.

EPA I materials produced the greatest stromal DoI and was significantly greater than that produced by EPA II ($P < 0.001$), EPA III ($P < 0.001$), and EPA IV ($P < 0.001$) materials (Fig. 7B and Table 4). Furthermore, damage to the corneal epithelium was also significantly greater than in control eyes or eyes exposed to EPA IV materials. EPA I materials also caused an increase in stromal thickness that was significantly greater than either EPA III ($P < 0.001$), EPA IV ($P < 0.001$), or control ($P < 0.001$), and showed a significantly thinner corneal epithelium compared to control-($P < 0.001$) and EPA IV-($P < 0.001$) treated corneas. Interestingly, corneas exposed to EPA I materials also showed a significant effect of exposure time on epithelial thickness ($P < 0.025$), stromal thickness ($P < 0.025$), epithelial DoI ($P < 0.05$), and stromal DoI ($P < 0.05$).

In contrast, EPA II materials caused significantly less stromal DoI compared to EPA I materials ($P < 0.001$), while causing significantly greater stromal DoI compared to EPA III-

(P < 0.05), EPA IV-(P < 0.005), and control-(P < 0.005) treated corneas. While epithelial DoI caused by EPA II materials was not significantly different from that of EPA I and EPA III materials, the epithelial DoI was significantly greater than that of EPA IV (P < 0.005) and control (P < 0.05) corneas. Although corneal stromal thickness was significantly greater in EPA II-exposed corneas compared to EPA IV-exposed corneas (P < 0.005) and control corneas (P < 0.001), this increase was not significantly different than the changes detected following exposure to either EPA I or EPA III materials. Similarly, epithelial thickness was significantly less than EPA IV-(P < 0.005) and control-(P < 0.05) exposed corneas, but not significantly different than EPA I-and EPA III-treated eyes.

Corneas exposed to EPA III materials showed significantly less stromal DoI compared to EPA I (P < 0.001) and EPA II (P < 0.005), but were not significantly different than EPA IV- or control-treated corneas. By comparison, epithelial DoI that was noted to be significantly increased with exposure time (P < 0.05) was greater than EPA IV (P < 0.005) and control (P < 0.05), but not significantly different than EPA II-or EPA I-exposed eyes. EPA III-exposed corneas also showed significantly increased stromal thickness compared to control (P < 0.05) and were significantly thinner than EPA I-treated corneas (P < 0.001), but were not significantly different than EPA II-or EPA IV-treated eyes. On the other hand, epithelial thickness was significantly thinner than EPA IV (P < 0.05) and control corneas (P < 0.05), but not significantly different than EPA I-or EPA II-treated eyes.

The GHS classification was similar to EPA, as shown in Fig. 7A and B, and Table 5. An exception was ethyl acetate, a GHS NC/EPA III material. Ethyl acetate produced an 11% stromal DoI and a 100% epithelial DoI at 24 h that were outside the range detected for the other GHS NC materials and overlapped those of GHS 2-classified materials.

3.4. EPA and GHS prediction models

The best prediction was obtained by measuring DoI at 24 h. Also, surfactants were excluded, as these require an alternative exposure strategy that has yet to be developed. Table 6 shows the proposed EPA and GHS prediction models. These models limit the measurement to a single time point taken at 24 hours post-exposure, which is a better predictor than 3 h for all measurements and significantly reduces the time and resources required to perform this test. It should be noted that the major difference between the EPA and GHS prediction models is based on significant damage to the epithelium, which is included in the EPA prediction model but not the GHS model. Since the GHS classification for live animal testing requires significant damage averaged over the first 3 days, we propose that this time would be adequate for the epithelium to recover unless there is also damage to the basement membrane, or stroma. Therefore, epithelial DoI does not need to be included in the prediction model. It should also be noted that stromal DoI was observed for every GHS-classified material. Thus, the proposed GHS prediction model excludes epithelial damage.

Based on these models, the EPA prediction model would correctly predict all category I materials, but misclassify one category II material (methyl thioglycolate), which was incorrectly classified as a category I material. All category III and IV materials would be correctly classified. For the GHS prediction model, all class 1 and 2A/2B materials would be

correctly classified. Additionally, all NC materials would be correctly classified, other than ethyl acetate, which would be classified as a class 2 irritant.

4. Discussion

This study identifies methods and prediction models for classifying ocular irritants using both the GHS and EPA classifications based on the histopathologic measurement of corneal DoI. While the inclusion of a histopathologic assessment of corneal injury has been widely recommended (ICCVAM, 2010) and is the subject of an OECD guideline for the collection and evaluation of eye tissues for enhancing the assessment of ocular irritation potential in organotypic models (OECD, 2018a), this is the first report that has identified clear and significant histopathologic differences between categories of known ocular irritants that have been classified based on recognized historical Draize test data. The findings in this report not only advance our ability to classify ocular irritants using an organotypic model but also provide potential insights into the underlying mechanisms driving different classification categories, as discussed below.

4.1. Histopathologic evaluation of the cornea

First, the recommendation of including histopathologic data in the assessment of ocular irritation has mainly focused on the use of standard histopathology methods, including formalin fixation, paraffin embedding, and routine histologic staining. This approach is problematic in that the ability to assess pathologic damage in corneal tissue generally requires a specialist in ocular pathology, with training beyond that required of anatomic pathologists. Even with such training, the identification of DoI remains highly speculative, particularly regarding changes in the corneal stroma using standard histologic staining methods. This problem is exemplified by the fact that the new OECD guidelines for assessing histopathologic damage to the cornea limits most if not all assessments to the corneal epithelium, which comprises seven of the nine subjective grading points for determining severity of injury (OECD, 2018a). Furthermore, epithelial damage as noted in the current study did not appear to play a role in determining the category of GHS-classified materials, all of which showed stromal damage de-pendent on the severity of the irritation class (GHS 1 ≫ GHS 2), and played a limited role in separating EPA III from IV materials, and no role in separating EPA I from II or III materials. While assessing epithelial injury is more convenient and is the focus of alternative eye irritation tests marketed as Epiocular, SkinEthic, and LabCyte, the critical differential between slight or no irritation and reversible or irreversible irritation appears to be damage to the corneal stroma, as identified in this study. The fact that these alternative tests focus only on epithelial damage and cannot be used to assess stromal damage may, in part, explain the limitation of these assays.

If histopathologic analysis of eye tissue is going to be of benefit for classifying ocular irritants, this study strongly indicates that it must be able to assess stromal damage. Such an assessment requires the use of specific probes to discriminate damaged from undamaged tissue. In this regard, it is noted that a recent alternative model, the Ex Vivo Eye Irritation Test (EVEIT), which uses O.C.T. imaging, has proven valuable for the categorization of ocular irritation based on both early and later responses (64–72 h) (Frentz et al., 2008;

Spoler et al., 2010; Spoler et al., 2015). While the EVEIT cannot be used to detect a difference in stromal DoI using O.C.T., this is most likely due to the limitation in O.C.T. detection of light scattering from the tissue, which can be af-fected not only by tissue damage but also by swelling of undamaged stroma. Furthermore, it should be noted that the EVEIT does not quantitatively measure DoI but only the quality of the O.C.T. signal from the corneal stroma.

4.2. Understanding mechanisms driving classification

EPA IV materials caused only slight damage to the epithelium (< 10%), whereas EPA I–III classified materials caused more damage to the epithelium (≥16%) as well as damage to the stroma. Similarly, GHS-classified materials (1 and 2A/2B) all caused damage to the stroma. Overall, these observations suggest that epithelial damage is a driver for only classifying EPA III materials. The reason underlying this finding is likely due to the fact that the corneal epithelium is being constantly replaced by progenitor cells from the limbus (located at the cornea/conjunctival border) (Dua et al., 1994), and damage to the epithelium is usually replaced within 24 h or, at most, 2–3 days (Bukowiecki et al., 2017). Furthermore, an epithelial wound causes a 5-fold increase in the proliferation of epithelial cells at the limbus and a 3-fold increase in the peripheral cornea, peaking approximately 24 h after wounding and providing substantial numbers of cells to quickly resurface the cornea (Ashby et al., 2014). Damage to the stroma also likely represents damage to the basement membrane, which plays a critical role in controlling corneal epithelial differentiation and repair mechanisms. Specifically, when the basement membrane is damaged, there is no longer a place for epithelial cells to attach to the corneal stroma via hemidesmosomal attachments, thus requiring replacement of the basement membrane, a delayed wound-healing response, and other downstream cellular and molecular consequences (Dua et al., 1994). As previously noted for the same-size corneal wound in rabbits, re-epithelization after lamellar keratectomy, which physically removes the basement membrane (5–7 days), takes longer than that following scrape injury (2–3 days), leaving the basement membrane intact (Essepian et al., 1990). It is therefore likely that chemicals that damage the corneal stroma also damage the basement membrane, causing delayed wound-healing responses that extend beyond 2–3 days and resulting in GHS classification.

Importantly, when the basement membrane is damaged, there is an influx of specific cytokines from both the tears and damaged epithelium, such as TGF-beta and PGF, into the stroma, promoting the activation of normally quiescent keratocytes to fibroblasts and myofibroblast. Depending on the level of cytokine stimulation, this alone can lead to the formation of fibrotic tissue and corneal haze or scarring (Torricelli et al., 2016). It was observed that ocular corrosives cause damage to the stroma of > 20%, which may correspond to damage that can induce the formation of scar tissue and permanent ocular defects; however, this requires further investigation.

Taken together, regeneration and remodeling of the corneal epithelial basement membrane appears to be a critical factor for determining whether the cornea heals with relative transparency or stromal fibrosis and opacity, and seems to be the major driver for classification of ocular irritation. In the future, how chemicals affect the basement membrane

and modify the epithelial wound-healing response may help predict the overall severity of the potential irritation response.

4.3. Limitations

A surfactant, tested as is, elicits a slightly different pattern of damage than other materials. Tween 20 (EPA III, GHS NC) caused only 16% damage to the epithelium and no damage to the stroma. On the other hand, 5% Triton X-100 (GHS 2A) caused almost complete damage of the epithelium and stroma, and was overpredicted as a corrosive. Surfactants are typically water soluble and may be diluted by tearing. Most nonanimal tests dilute surfactants as a class prior to testing, including BCOP (OECD, 2017) and OptiSafe (Vij et al., 2019). For this assay, it may be that additional work as well as dilution are required to optimize the dosing procedures for surfactants. Besides 5% Triton X-100, all GHS corrosives have a stromal DoI of 38% or more. Methyl thioglycolate, a GHS 1 (corrosive)/EPA II (reversible), exhibited a stromal DoI of 38%. A review of the in vivo data for this chemical (Adriaens et al., 2014; ECETOC, 1998) indicates that the GHS classification is driven by the severity of the corneal response and not the reversibility of response. The next severe response at a stromal DoI of 39% was the EPA 1/GHS 1 cyclohexanol. Additional studies are required to determine whether there is an exact cut-off for stromal DoI to differentiate reversible from irreversible damage, as measured by this procedure. Out of an abundance of caution, we have preliminarily set the cut-off for ocular corrosives in our model at a stromal DoI of 20%, which means that there would be one GHS overprediction as corrosive (the surfactant, 5% Triton X-100, previously discussed) and two EPA overpredictions as corrosive (Triton X-100 and methyl thioglycolate).

Ethyl acetate, with a stromal DoI of 12%, is overpredicted as GHS classified. Both an older in vivo database (ECETOC) and a more current study indicate that this material is a GHS NC, and the more current study obtained from a third party indicates that this material is a borderline GHS positive. In the newer study, one of three animals had scores that would result in a GHS classification, but a second animal did not. Given the variability of in vivo studies, if this study were to be repeated, this material would likely be classified as an irritant by the GHS system. Besides ethyl acetate, all GHS NC substances had a stromal DoI of 0%.

While one ocular corrosive (tetraethylene glycol diacrylate) showed almost no measurable response at 3 h, there was almost complete loss of stromal cell viability as measured by the ability to maintain actin, an ATP-dependent process, at 24 h. This material is a DNA cross-linker and may act as a fixative (Mabilleau et al., 2006). Previous studies of nitrogen mustards have identified a similar delay in cellular damage associated with DNA cross-linking (Charkoftaki et al., 2018). Similar delayed injury was noted in live animal studies for other cross-linking materials such as aldehydes (Maurer et al., 2001b) as well as bleaches (Maurer et al., 2001a). Alternative tests that rely on short-term post-exposure intervals < 24 h may also be subject to similar limitations.

4.4. Conclusion

We present a method and prediction model for reversible ocular irritation based on the histopathologic measurement of eye DoI after a 24 hour organ culture and viability staining associated with specific types of damage within the EPA and GHS classifications. EPA classification is first measured at 24 h; therefore, damage to the epithelium is relevant. The first relevant measurement for the GHS is damage averaged over the first 3 days, when there is sufficient time for recovery of the epithelium, unless the basement membrane and stroma are damaged. Therefore, from both a mechanistic and statistical perspective, we conclude that GHS classification is best related to damage to the stroma and perhaps the basement membrane.

Prospective studies comparing this approach with damage measured in vivo for a broad range of chemicals, representing the different physiochemical classes of ocular irritants of all hazard classes, are needed to more clearly establish the proposed methods and prediction models.

Acknowledgments

Supported in part by an unrestricted grant from Research to Prevent Blindness, Inc, and an NIEHS Small Business Innovative Research Grant. Research reported in this publication was supported by the National Institute of Environmental Health Sciences of the National Institutes of Health under Award Number R44ES025501. The content is solely the responsibility of the authors and does not necessarily represent the official views of the National Institutes of Health.

References

Adriaens E, Barroso J, Eskes C, Hoffmann S, McNamee P, Alepee N, Bessou-Touya S, De Smedt A, De Wever B, Pfannenbecker U, Tailhardat M, Zuang V, 2014 Retrospective analysis of the Draize test for serious eye damage/eye irritation: importance of understanding the in vivo endpoints under UN GHS/EU CLP for the development and evaluation of in vitro test methods. Arch. Toxicol 88, 701–723. [PubMed: 24374802]

Ashby BD, Garrett Q, Willcox MDP, 2014 Corneal injuries and wound healing—review of processes and therapies. Austin J. Clin. Ophthal 1, 1–25.

Barroso J, Pfannenbecker U, Adriaens E, Alepee N, Cluzel M, De Smedt A, Hibatallah J, Klaric M, Mewes KR, Millet M, Templier M, McNamee P, 2017 Cosmetics Europe compilation of historical serious eye damage/eye irritation in vivo data analysed by drivers of classification to support the selection of chemicals for development and evaluation of alternative methods/strategies: the Draize eye test reference database (DRD). Arch. Toxicol 91, 521–547. [PubMed: 26997338]

Bruner LH, 1992 Alternatives to the use of animals in household product and cosmetic testing. J. Am. Vet. Med. Assoc 200, 669–673. [PubMed: 1568909]

Bukowiecki A, Hos D, Cursiefen C, Eming SA, 2017 Wound-healing studies in cornea and skin: parallels, differences and opportunities. Int. J. Mol. Sci 18.

Charkoftaki G, Jester JV, Thompson DC, Vasiliou V, 2018 Nitrogen mustard-induced corneal injury involves the sphingomyelin-ceramide pathway. Ocul. Surf 16, 154–162. [PubMed: 29129753]

Choksi N, Daniel A, Lebrun SJ, Nguyen M, DeGeorge G, Willoughby JA, Casey W, Aleen D, 2017 Abstract, Performance of the OptiSafe Ocular Irritation Assay in a Three-Laboratory Validation Study. Society of Toxicology Annual Meeting.

Draize JH, Woodard G, Calgary H, 1944 Methods for the study of irritation and toxicity of substances applied topically to the skin and mucous membranes. J. Pharmacol. And Exp. Ther 82, 377–390.

Dua HS, Gomes JA, Singh A, 1994 Corneal epithelial wound healing. Br. J. Ophthalmol 78, 401–408. [PubMed: 8025077]

ECETOC, 1998. Eye irritation: reference chemicals data bank. In: Chemicals, 2nd ed. (E.C.f.E.a.T.o. (Ed.), Brussels).

Essepian JP, Wei F, Hildesheim J, Jester JV, 1990 Comparison of corneal epithelial wound healing rates in scrape vs. lamellar keratectomy injury. Cornea 9, 294–298. [PubMed: 2078958]

Frentz M, Goss M, Reim M, Schrage NF, 2008 Repeated exposure to benzalkonium chloride in the Ex Vivo Eye Irritation Test (EVEIT): observation of isolated corneal damage and healing. Altern. Lab. Anim 36, 25–32. [PubMed: 18333712]

Gautheron P, Giroux J, Cottin M, Audegond L, Morilla A, Mayordomo-Blanco L, Tortajada A, Haynes G, Vericat JA, Pirovano R, Gillio Tos E, Hagemann C,Vanparys P, Deknudt G, Jacobs G, Prinsen M, Kalweit S, Spielmann H, 1994 Interlaboratory assessment of the bovine corneal opacity and permeability (BCOP) assay. Toxicol. in Vitro 8, 381–392. [PubMed: 20692929]

Grune B, Herrmann S, Dorendahl A, Skolik S, Behnck-Knoblau S, Box R, Spielmann H, 2000 The ZEBET database on alternative methods to animal experiments in the internet–a concrete contribution to the protection of animals. ALTEX 17, 127–133. [PubMed: 11105194]

H.R.2790, 2017 Humane Cosmetics Act 115th Congress. Rep. McSally, Martha [R-AZ-2] (Introduced 06/06/2017). [online] Available at. https://www.congress.gov/bill/115th-congress/house-bill/2790.

Hamrah P, Alipour F, Jiang S, Sohn JH, Foulks GN, 2011 Optimizing evaluation of Lissamine green parameters for ocular surface staining. Eye (Lond) 25, 1429–1434. [PubMed: 21836630]

Humane Society, 2017 Timeline: Cosmetics Testing on Animals: The Humane Society of the United States. [online] Available at. http://www.humanesociety.org/issues/cosmetic_testing/timelines/timeline-cosmetics-testing-on-animals.html, Accessed date: December 2019.

ICCVAM, 2009 Independent Scientific Peer Review Panel Report: Evaluation of the Validation Status of Alternative Ocular Safety Testing Methods and Approaches. http://iccvam.niehs.nih.gov/docs/ocutox_docs/OcularPRPRept2009.pdf.

ICCVAM, 2010 ICCVAM Test Method Evaluation Report: Current Validation Status of a Proposed In Vitro Testing Strategy for U.S. Environmental Protection Agency Ocular Hazard Classification and Labeling of Antimicrobial Cleaning Products.

Lebrun SJ, Choksi N, Daniel A, Allen D, Casey W, 2019 Prevalidation of the OptiSafeTM Ocular Irritaion Assay for the Detection of Ocular Corrosives. NICEATM, Society of Toxicology Annual Meeting.

Mabilleau G, Stancu IC, Honore T, Legeay G, Cincu C, Basle MF, Chappard D, 2006 Effects of the length of crosslink chain on poly(2-hydroxyethyl methacrylate) (pHEMA) swelling and biomechanical properties. J. Biomed. Mater. Res. A 77, 35–42. [PubMed: 16345096]

Maurer JK, Molai A, Parker RD, Li L, Carr GJ, Petroll WM, Cavanagh HD, Jester JV, 2001a Pathology of ocular irritation with bleaching agents in the rabbit low-volume eye test. Toxicol. Pathol 29, 308–319. [PubMed: 11442017]

Maurer JK, Molai A, Parker RD, Li LI, Carr GJ, Petroll WM, Cavanagh HD, Jester JV, 2001b Pathology of ocular irritation with acetone, cyclohexanol, parafluoroaniline, and formaldehyde in the rabbit low-volume eye test. Toxicol. Pathol 29, 187–199. [PubMed: 11421486]

OECD, 2017 Test no. 437: bovine corneal opacity and permeability test method for identifying (i) chemicals inducing serious eye damage and (ii) chemicals not requiring classification for eye irritation or serious eye damage. In: Editor (Ed.)^ (Eds.) In: Book Test No. 437: Bovine Corneal Opacity and Permeability Test Method for Identifying (i) Chemicals Inducing Serious Eye Damage and (ii) Chemicals Not Requiring Classification for Eye Irritation or Serious Eye Damage, Paris, 10.1787/9789264203846-en.

OECD, 2018a Test No. 160: Guidance Document on the Collection of Eye Tissues for Histological Evaluation and Collection of Data. OECD Publishing, Paris.

OECD, 2018b Test No. 492: Reconstructed Human Cornea-Like Epithelium (RhCE) Test Method for Identifying Chemicals Not Requiring Classification and Labelling for Eye Irritation or Serious Eye Damage. OECD Publishing, Paris 10.1787/9789264242548-en.

Rowan AN, 1984 The future of animals in research and training. The search for alternative. Fundam. Appl. Toxicol 4, 508–516. [PubMed: 6479495]

S.697, 2015 Frank R. Lautenberg Chemical Safety for the 21st Century Act. 114th Congress. [online]. https://www.congress.gov/bill/114th-congress/senate-bill/697.

SB1249, 2018. California cruelty-free cosmetics act. Civil Code 1934 (1939), 1935.

Senate Joint Resolution 22, 2014 Introduced by Senator Block. http://leginfo.legislature.ca.gov/faces/billNavClient.xhtml?bill_id=201320140SJR22&search_keywords.

Spoler F, Frentz M, Schrage NF, 2010 Towards a new in vitro model of dry eye: the ex vivo eye irritation test. Dev. Ophthalmol 45, 93–107. [PubMed: 20502030]

Spoler F, Kray O, Kray S, Panfil C, Schrage NF, 2015 The ex vivo eye irritation test as an alternative test method for serious eye damage/eye irritation. Altern. Lab. Anim 43, 163–179. [PubMed: 26256395]

Torricelli AA, Santhanam A, Wu J, Singh V, Wilson SE, 2016 The corneal fibrosis response to epithelial-stromal injury. Exp. Eye Res 142, 110–118. [PubMed: 26675407]

UN, 2011 United Nations Globally Harmonized System of Classification and Labelling of Chemicals (GHS), ST/SG/AC.10/30 Rev 4, Part 3 Health Hazards–Chapter 3.3 Serious Eye Damage/Eye Irritation. United Nations Publications, New York & Geneva http://www.unece.org/trans/danger/publi/ghs/ghs_rev04/04files_e.html.

Vij P, Lebrun SJ, DeGeorge G, 2019 Classification of EPA Ocular Irritants and Non-Irritants by the OptiSafeTM and EIT Test Methods. Society of Toxicology Annual Meeting.

Weil CS, Scala RA, 1971 Study of intra-and interlaboratory variability in the results of rabbit eye and skin irritation tests. Toxicol. Appl. Pharmacol 19, 276–360. [PubMed: 5570968]

Wilson SL, Ahearne M, Hopkinson A, 2015 An overview of current techniques for ocular toxicity testing. Toxicology 327, 32–46. [PubMed: 25445805]

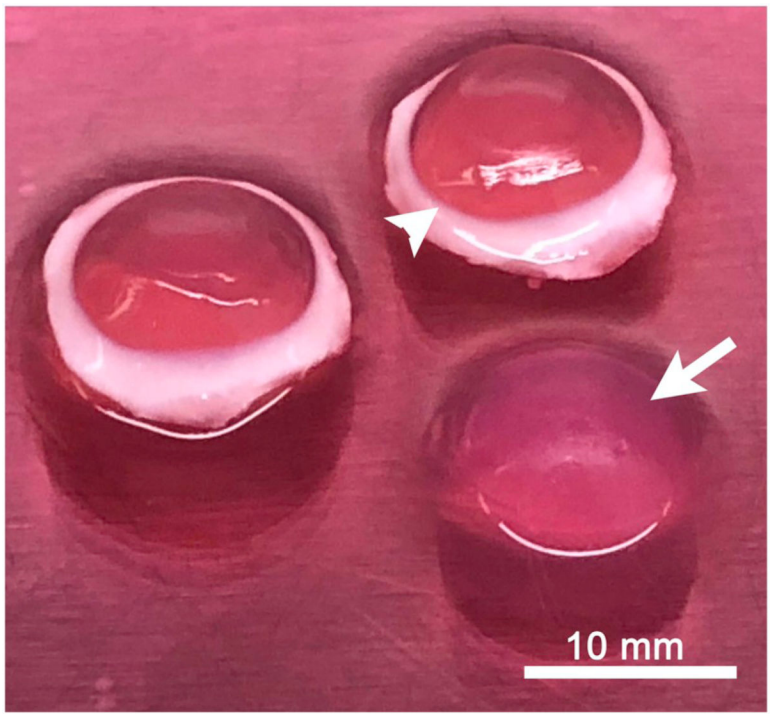

Fig. 1.
Rabbit cornea organ culture. Corneas were placed onto agar posts (arrow), and the medium was added up to the corneoscleral junction (Limbus, arrowhead).

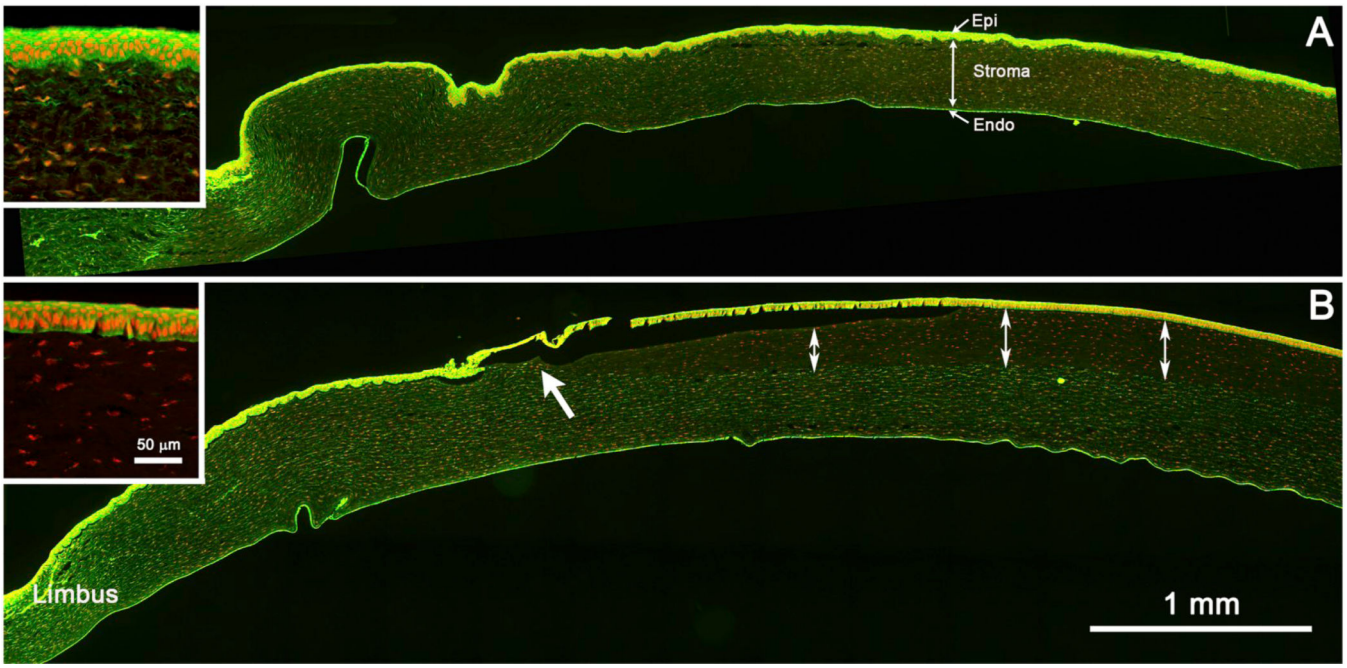

Fig. 2.

Tiled image of phalloidin (green) and nuclear (red) staining of a rabbit cornea after 3 hours exposure to sterile water (A, control), and methyl thioglycolate (B, EPA II). The section covers the limbal region to the left (Limbus) and the central cornea to the right. Control cornea shows intense phalloidin staining of the corneal epithelium (Epi), weaker staining of the corneal keratocytes (Stroma), and strong staining of the endothelium (Endo). Inset shows higher magnification of the corneal epithelial and stromal staining. A cornea exposed to methyl thioglycolate shows loss of phalloidin staining of the keratocytes (double-headed arrows), starting in the paracentral cornea (arrow) and extending to the central cornea. Inset shows the loss of both corneal epithelial and keratocyte phalloidin staining. (For interpretation of the references to colour in this figure legend, the reader is referred to the web version of this article.)

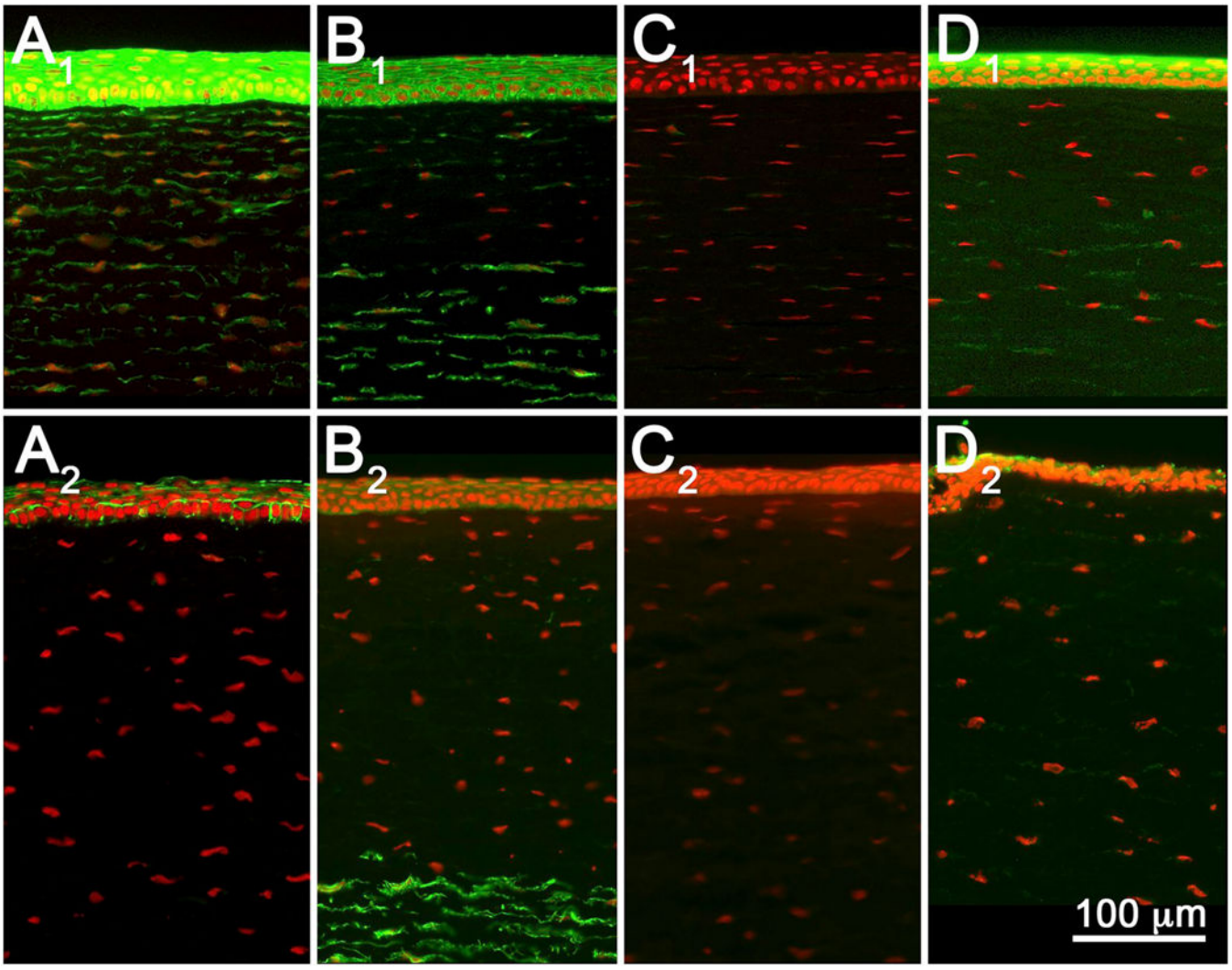

Fig. 3.

Tissue sections from rabbit corneas exposed to EPA I materials tetraethylene glycol diacrylate (A), cyclohexanol (B), lactic acid (C), and benzalkonium chloride (D), and fixed at 3-(A_1–D_1) or 24 h (A_2–D_2) post-exposure. While 3 hours post-exposure showed variable stromal DoI, 24 hours post-exposure showed extensive stromal DoI by all materials. Note that tetraethylene glycol diacrylate showed no damage at 3 h (A_1) but extensive damage by 24 h (A_2).

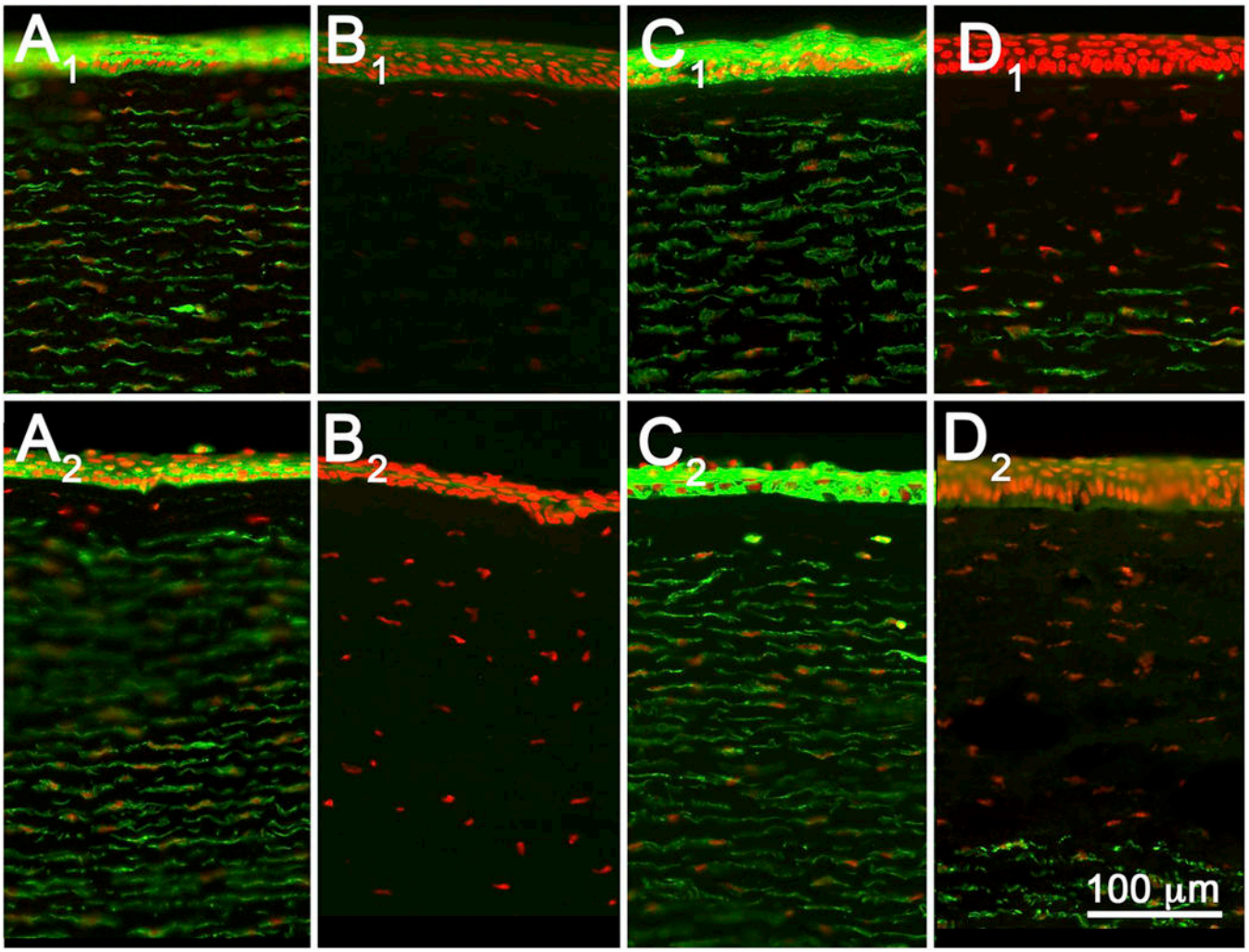

Fig. 4.

Tissue sections from rabbit corneas exposed to EPA II materials 1-octanol (A), Triton X-100 (B), acetone (C), and methyl thioglycolate (D), and fixed at 3-(A_1–D_1) or 24 h (A_2–D_2) post-exposure.

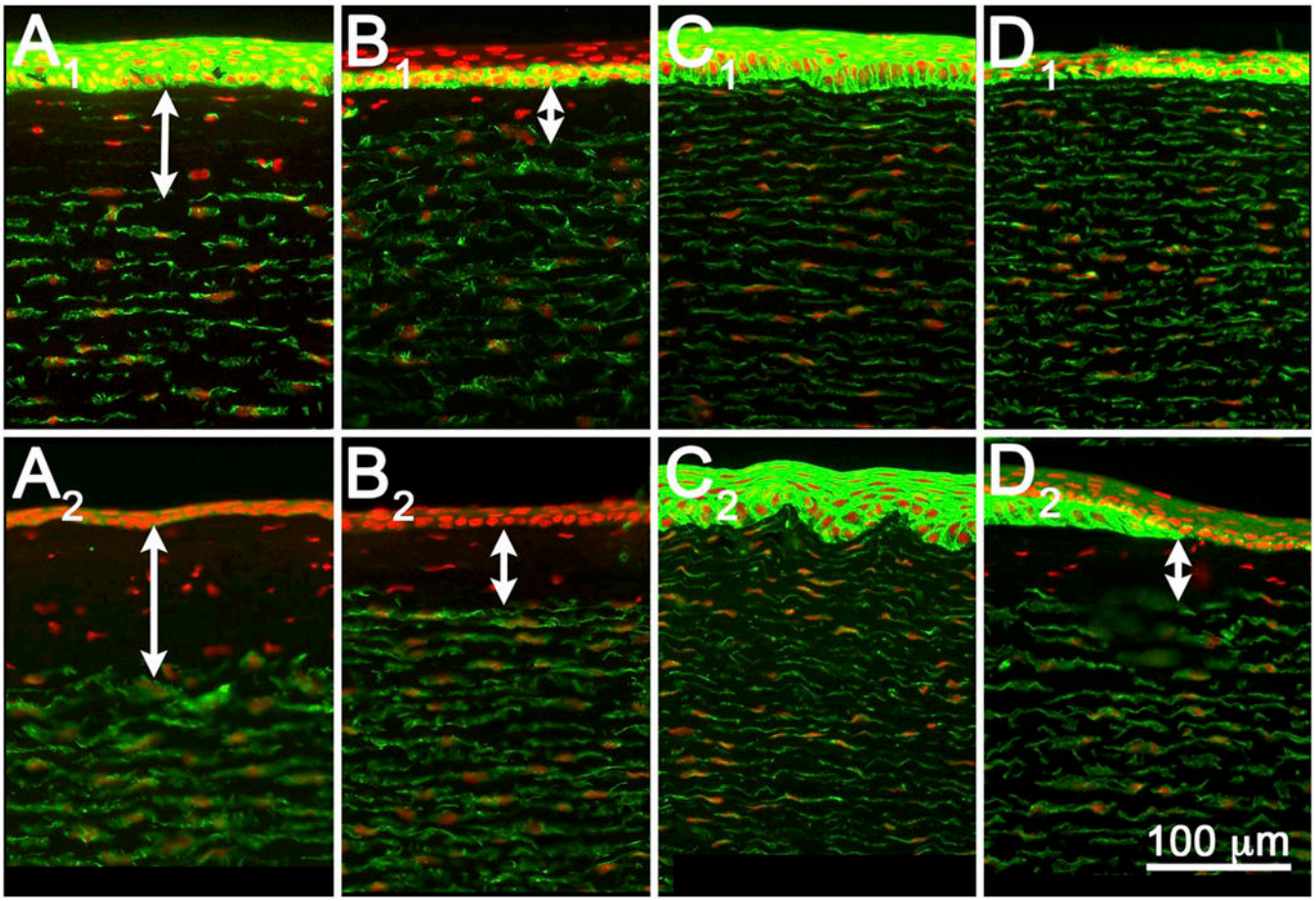

Fig. 5.

Tissue sections from rabbit corneas exposed to EPA category III materials ethyl acetate (a), 3-chloroproprionitrile (b), Tween 20 (C), and isopropanol (D), and fixed at 3-(A_1–D_1) or 24 hours (A_2–D_2) post-exposure.

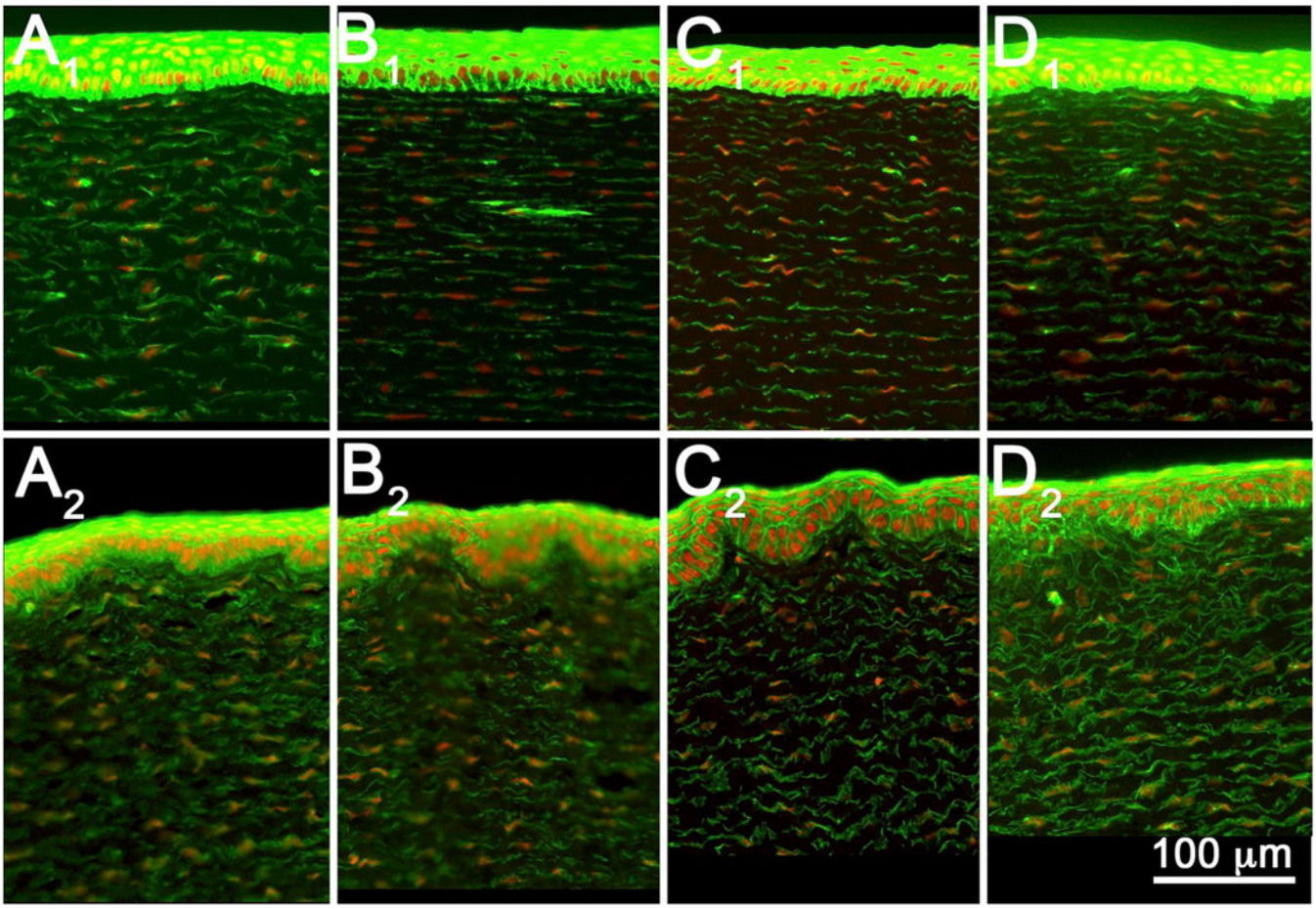

Fig. 6.

Tissue sections from rabbit corneas exposed to EPA category IV materials n-hexyl bromide (A), 2-ethylhexyl thioglycolate (B), Tween 80 (C), and isooctyl acrylate (D), and fixed at 3- (A_1–D_1) or 24 hours (A_2–D_2) post-exposure.

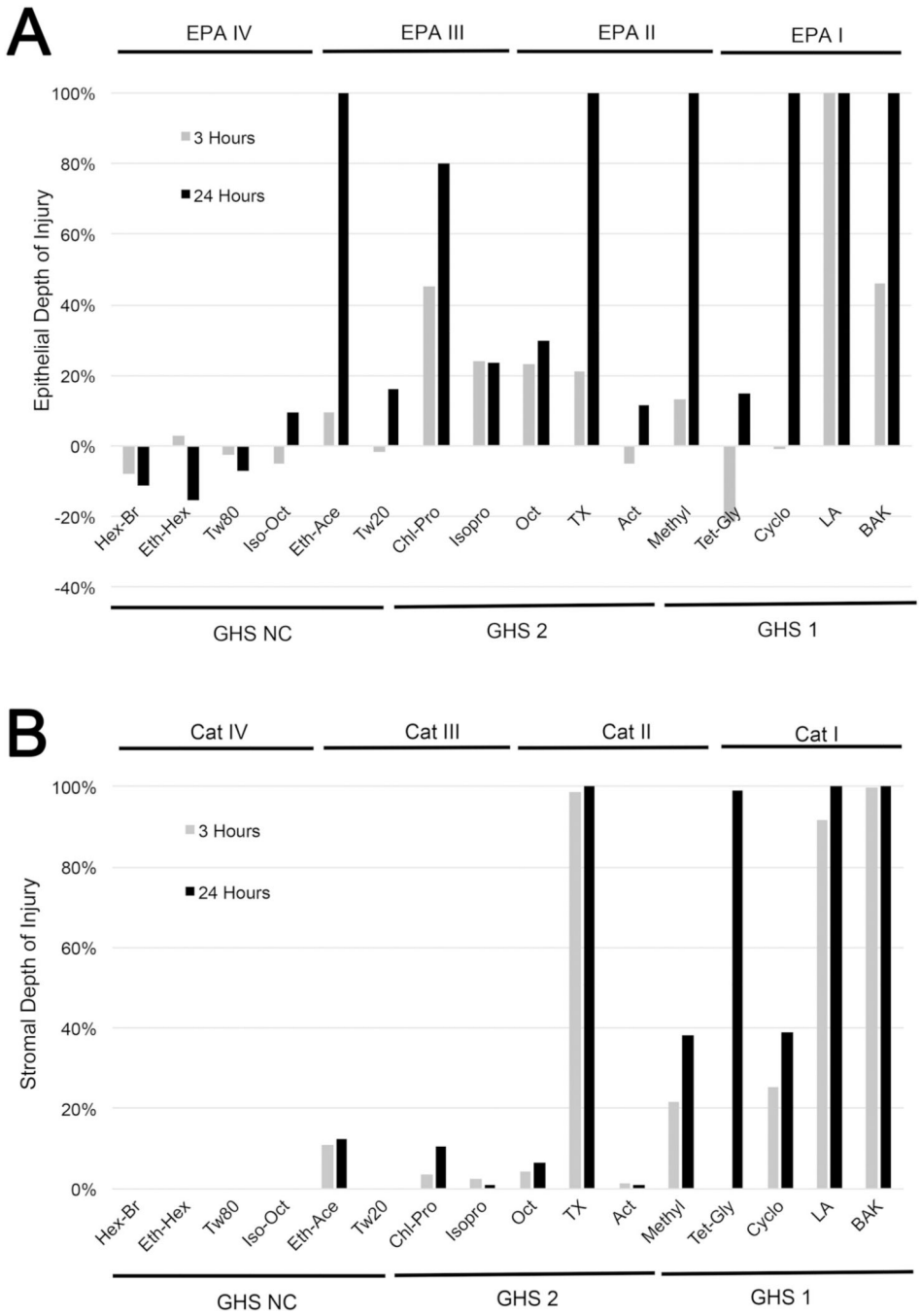

Fig. 7.

Graph of epithelial (A) and stromal (B) DoI measured at 3 h (gray bars) and 24 h (black bars) after exposure to EPA I, II, III, and IV materials or GHS NC, 2A/ 2B, and 1 materials.

Table 1

Test material concentrations and abbreviations.

Chemical name	Abbreviation	CASRN	Code number	Supplier	Purity stated by supplier	EPA class.	GHS class.	In Vivo purity
Isooctyl acrylate	Iso-Oct	29590-42-9	16	Sigma-Aldrich	> 90	IV[a]	NC[a]	> 99
2-Ethylhexyl thioglycolate	Eth-Hex	7659-86-1	6	Sigma-Aldrich	≥95	IV[a]	NC[a]	99.4
n-Hexyl bromide	Hex-Br	111-25-1	4	Sigma-Aldrich	98	IV[a]	NC[a]	> 98.5
Tween 80	Tw80	9005-65-6	13	Sigma-Aldrich	-	IV[c]	NC[c]	–
Tween 20	Tw20	9005-64-5	9	Sigma-Aldrich	≥40	III[a]	NC[a]	98
Ethyl Acetate	Eth-Ace	141-78-6	1	Sigma-Aldrich	99.8	III[a]	NC[a]	99
3-Chloropropionitrile	Chl-Pro	542-76-7	5	Sigma-Aldrich	98	III[a]	2B[a]	99.9
Isopropanol	Isopro	67-63-0	12	Sigma-Aldrich	99.5	III[a]	2A[a]	99.9
1-Octanol	Oct	111-87-5	2	Millipore	≥98	II[a]	2A[a]	> 99
Acetone	Act	67-64-1	7	Sigma-Aldrich	≥99.5	II[a]	2A[a]	99
Triton X-100 (5%)	TX	9002-93-1	3	Sigma-Aldrich	–	II[a]	2A[a]	98
Methyl thioglycolate	Methyl	2365-48-2	15	Sigma-Aldrich	95	II[a]	I[a]	99.7
Lactic acid	LA	50-21-5	11	Sigma-Aldrich	~90	I[b]	I[b]	–
Cyclohexanol	Cyclo	108-93-0	10	Sigma-Aldrich	99	I[a]	I[a]	97
Benzalkonium chloride (1%)	BAK	63449-41-2	14	Sigma-Aldrich	≥95	I[a]	I[a]	98
Tetraethylene glycol diacrylate	Tet-Gly	17831-71-9	8	Sigma-Aldrich	≥87	I[c]	I[c]	–

[a] ECETOC Technical Report No. 48 (1998).

[b] NICEATM.

[c] Cosmetics Europe.

Table 2

3 Hours post exposure.

Material	Classification		Epithelial thickness		Stromal thickness		Epithelial DoI		Stromal DoI	
	GHS	EPA	Mean	SD	Mean	SD	Mean	SD	Mean	SD
n-Hexyl bromide	NC	IV	39.2	3.4	408.4	78.1	−8%	9%	0%	0%
2-Ethylhexyl thioglycolate	NC	IV	35.3	4.9	335.1	47.5	3%	13%	0%	0%
Tween 80	NC	IV	37.3	4.9	394.5	58.9	−2%	14%	0%	0%
Isooctyl acrylate	NC	IV	38.2	0.9	497.1	115.7	−5%	3%	0%	0%
Ethyl acetate	NC	III	32.9	8.6	540.4	90.7	10%	24%	11%	1%
Tween 20	NC	III	37.0	5.0	369.6	58.6	−2%	14%	0%	0%
3-Chloropropionitrile	2B	III	20.0	13.8	492.7	61.0	45%	38%	3%	1%
Isopropanol	2A	III	27.6	0.6	539.3	89.2	24%	2%	2%	4%
1-Octanol	2A	II	28.0	3.7	466.6	19.7	23%	10%	4%	2%
Triton X-100 5%	2A	II	28.6	7.4	612.9	122.2	21%	20%	99%	1%
Acetone	2A	II	38.2	4.7	521.5	79.7	−5%	13%	1%	3%
Methyl thioglycolate	1	II	31.5	8.7	642.6	25.9	13%	24%	22%	9%
Tetraethylene glycol diacrylate	1	I	44.2	5.7	506.5	72.5	−21%	16%	0%	0%
Cyclohexanol	1	I	36.7	12.0	717.5	127.4	−1%	33%	25%	7%
Lactic acid	1	I	0.0	0.0	438.2	76.0	100%	0%	92%	14%
Benzallkonium chloride 1%	1	I	19.6	7.6	708.3	30.7	46%	21%	100%	0%
Water	NA	NA	36.4	5.8	348.2	48.5	NA	NA	NA	NA

Table 3

24 Hours post exposure.

Material	Classification		Epithelial thickness		Stromal thickness		Epithelial DoI		Stromal DoI	
	GHS	EPA	Mean	SD	Mean	SD	Mean	SD	Mean	SD
n-Hexyl bromide	NC	IV	43.2	3.5	766.7	323.9	−11%	9%	0%	0%
2-Ethylhexyl thioglycolate	NC	IV	44.7	1.4	414.7	48.1	−15%	4%	0%	0%
Tween 80	NC	IV	41.5	3.5	379.2	45.0	−7%	9%	0%	0%
Isooctyl acrylate	NC	IV	35.0	6.6	356.2	37.9	10%	17%	0%	0%
Ethyl acetate	NC	III	0.0	0.0	573.0	43.8	100%	0%	12%	9%
Tween 20	NC	III	32.4	4.9	315.1	10.0	16%	13%	0%	0%
3-Chloropropionitrile	2B	III	7.7	0.9	667.5	269.4	80%	2%	11%	0%
Isopropanol	2A	III	29.6	13.7	501.9	81.7	24%	35%	1%	2%
1-Octanol	2A	II	27.3	6.1	500.8	8.0	30%	16%	6%	2%
Triton X-100 5%	2A	II	0.0	0.0	879.9	256.6	100%	0%	100%	0%
Acetone	2A	II	34.2	4.5	531.9	99.4	12%	12%	1%	1%
Methyl thioglycolate	1	II	0.0	0.0	613.2	12.5	100%	0%	38%	7%
Tetraethylene glycol diacrylate	1	I	33.0	8.5	719.9	59.9	15%	22%	99%	1%
Cyclohexanol	1	I	0.0	0.0	650.8	135.5	100%	0%	39%	13%
Lactic Acid	1	I	0.0	0.0	625.2	95.9	100%	0%	100%	0%
Benzallkonium chloride 1%	1	I	0.0	0.0	943.0	82.5	100%	0%	100%	0%
Water	NA	NA	38.8	4.4	358.4	22.0	NA	NA	NA	NA

Table 4

Comparison between EPA categories and time.

EPA category	Time	Epithelial thickness			Stromal thickness			Epithelial DoI			Stromal DoI		
		Mean	SD	P-value*	Mean	SD	P-value	Mean	SD	P-value	Mean	SD	P-value
Cat IV	3	37.5	1.7	I^{c}, II^{c}, III^{b}	408.8	66.9	I^{c}, II^{b}	−3%	5%	I^{c}, II^{b}, III^{b}	0%	0%	I^{c}, II^{b}
	24	41.1	4.3		479.2	193.2		−6%	11%		0%	0%	
	P-value	NS			NS			NS			NS		
Cat III	3	29.4	7.4	IV^{b}, Con^{a}	485.5	80.4	I^{c}, Con^{a}	19%	20%	IV^{b}, Con^{a}	4%	5%	I^{c}, II^{a}
	24	17.4	16.0		514.4	149.2		55%	41%		6%	3%	
	P-value	NS			NS			< 0.05			NS		
Cat II	3	31.6	4.7	IV^{b}, Con^{a}	560.9	81.3	IV^{b}, Con^{c}	13%	13%	IV^{b}, Con^{a}	31%	46%	I^{c}, III^{a}, IV^{b}, Con^{b}
	24	15.4	18.0		631.4	172.3		60%	46%		36%	45%	
	P-value	< 0.025			NS			< 0.05			NS		
Cat I	3	25.1	19.7	IV^{c}, Con^{c}	592.6	141.7	III^{c}, IV^{c}, Con^{c}	31%	54%	IV^{c}, Con^{c}	54%	14%	II^{c}, III^{c}, IV^{c}, Con^{c}
	24	8.3	16.5		734.7	144.5		79%	43%		85%	30%	
	P-value	< 0.025			<0.025			<0.05%			< 0.05		
Control	3	36.4	5.8	I^{c}, II^{a}, III^{b}	348.2	48.5	I^{c}, II^{c}, III^{a}	NA	NA	I^{c}, II^{a}, III^{a}	NA	NA	I^{c}, II^{a}
	24	38.8	4.4		358.4	22.0		NA	NA		NA	NA	
	P-value	NS			NS								

Con = Control.

*Comparing each Category to the others.

^{a}P < 0.05.

^{b}P < 0.005.

^{c}P < 0.001.

Table 5

Comparison between GHS categories and time.

EPA category	Time	Epithelial thickness			Stromal thickness			Epithelial DoI			Stromal DoI		
		Mean	SD	P-value*	Mean	SD	P-value	Mean	SD	P-value	Mean	SD	P-value
NC	3	36.6	2.3	1^{c}, 2^{a}	424.2	78.6	1^{c}, 2^{c}	−1%	6%	1^{c}, 2^{a}	2%	4%	1^{c}
	24	32.8	16.8		467.5	171.4		15%	43%		2%	5%	
	P-value	NS			NS			NS			NS		
2A/2B	3	28.5	6.5	1^{a}, NC^{a}, Con^{a}	526.6	55.7	1^{c}, NC^{b}, Con^{c}	22%	18%	1^{a}, NC^{a}, Con^{a}	22%	43%	1^{c}
	24	19.7	15.0		616.4	162.5		49%	39%		24%	43%	
	P-value	NS			NS			< 0.05			NS		
1	3	26.4	17.3	2^{a}, NC^{c}, Con^{c}	602.6	124.7	2^{c}, NC^{c}, Con^{c}	27%	47%	2^{a}, NC^{c}, Con^{c}	48%	45%	2^{c}, NC^{c}, Con^{c}
	24	6.6	14.8		710.4	136.4		83%	38%		75%	33%	
	P-value	<0.025			NS			< 0.05	NA		NS		1^{c}
Control	3	36.4	5.8	1^{c}, 2^{a}	348.2	48.5	1^{c}, 2^{a}	NA	NA	1^{c}, 2^{a}	NA	NA	1^{c}
	24	38.8	4.4		358.4	22.0		NA	NA		NA	NA	
	P-value	NS			NS								

Con = Control.

*Comparing each Category to the others.

^{a}P < 0.05.

^{b}P < 0.005.

^{c}P < 0.001.

Table 6

EPA and GHS prediction modeles.

EPA category	Stromal DoI	Epithelial DoI	GHS category	Stromal DoI
IV	0%	≤10%	NC	0%
III/II	> 0–20%	> 10%	2B/2A	> 0–20%
I	>20%	N/A	1	>20%